T. Curran, now director of the Aero Propulsion and Power Directorate of the Wright Laboratory, that took place in 1992. His continuing interest in the project since then has also been of great value.

References

[1]Heiser, W. H., McClure, W. B., and Wood, C. W., "Simulating Heat Addition via Mass Addition in Constant Area Compressible Flows," *AIAA Journal*, Vol. 33, No. 1, 1995, pp. 167–171.

[2]Shapiro, A. H., *The Dynamics and Thermodynamics of Compressible Fluid Flow*, Ronald, New York, 1953, Chap. 8.

[3]Heiser, W. H., and Pratt, D. T., *Hypersonic Airbreathing Propulsion*, AIAA Education Series, AIAA, Washington, DC, 1994, Chap. 6.

[4]Pratt, D. T., and Heiser, W. H., "Isolator-Combustor Interaction in a Dual-Mode Scramjet Engine," AIAA Paper 93-0358, Jan. 1993.

[5]Van Leer, B., "Flux-Vector Splitting for the Euler Equations," *Lecture Notes in Physics*, Vol. 170, Springer–Verlag, New York, 1982, pp. 507–512.

Dusty Shock Flow with Unstructured Adaptive Finite Elements and Parcels

S. Sivier* and E. Loth[†]
University of Illinois at Urbana–Champaign, Urbana, Illinois 61801
J. Baum[‡]
Science Applications International Corporation, McLean, Virginia 22102
and
R. Löhner[§]
George Mason University, Fairfax, Virginia 22030

I. Introduction

WHEN solving the compressible two-phase equations, the gas as a continuum is best represented by an Eulerian description, i.e., the gas characteristics are calculated at fixed points within the flow. The particles (or droplets), however, may be modeled by either an Eulerian description (in the same manner as the gas flow), or a Lagrangian description (where individual particle groups are monitored and tracked in the flow). Herein, the former will be referred to as an Eulerian–Eulerian (E–E) treatment, whereas the latter will be defined as an Eulerian–Lagrangian (E–L) treatment. Recently, Sivier et al.[1] developed an E–E method using an unstructured grid finite element method–flux corrected transport (FEM–FCT) flow solver in order to examine shock wave attenuation in dusty shock flows. FEM–FCT was designed to be able to capture flow features with large gradients, such as those that occur in density near shocks. Whereas a Lagrangian approach offers many potential advantages, this method also creates potential problems that should be addressed by the model. For instance, large numbers of particles may cause a Lagrangian analysis to be memory intensive (this may be partially offset by using parcels, each of which represents a number of particles in the flow). In addition, continuous mapping and remapping of particles to their respective elements may increase computational requirements, particularly for unstructured grids.

Both E–E and E–L descriptions have been used widely on structured grids,[2,3] but this research seeks a comparative study between these two approaches when coupled with a dynamically adaptive unstructured finite element method with a novel parcel adaptive technique. The objective of the present study was to formulate and develop an E–L method with an adaptive grid FEM–FCT flow solver that is computationally efficient. This method was used to predict a particle laden shock wave attenuation as a test case and to compare performance characteristics (computation speed, memory, and accuracy) with an E–E implementation[1] that also includes adaptive unstructured grids.

II. Numerical Method

One particular two-phase flow that includes two-way coupling of interphase momentum transport and compressible flow effects is dusty shock attenuation, which is typically modeled with E–E formulations.[1,4,5] In such a flow, the particle densities are typically two to three orders of magnitude higher than that of the carrier gas, such that particle mass loadings of order unity yield significant modification of the gas flow behavior but with corresponding negligible volume loadings (e.g., less than 1%), such that particle–particle interactions and volume displacement effects can be typically eliminated. We will herein restrict ourselves to such flow conditions. The gas equations used in the current study are the Euler equations with non-homogenous source terms added to represent the interphase momentum and energy transfer.[1,4,5]

Dynamic unstructured grid adaption was employed to optimize the distribution of nodal points by continually refining areas with high gradients of gas density and coarsening areas of low gradients of gas density, where the maximum level of refinement (LOR) is preset. Since we are interested in computing dilute particle flows of negligible volume fraction (but significant mass fraction) with particle diameters on the order of several microns, the present technique assumes particle effects on gas pressures and particle–particle interactions are negligible, and particles are spherical and inert. In addition, since the flow is nonreacting and the particles are relatively small, radiation and gravitational effects are neglected.

The Lagrangian particle description was implemented by tracking individual groups of particles, referred to as parcels.[6,7] The previous timestep's gas characteristics for a host element (the element that contains a given parcel) are linearly interpolated to each parcel coordinate to determine the momentum and energy interphase coupling terms D_i and Q as follows[5]:

$$D_i = \frac{\pi}{8}\frac{\phi_k N_p}{A_e}\rho C_D|u_i - u_{pi}|(u_i - u_{pi})d^2$$

$$Q = \pi d^2 \frac{\phi_k N_p}{A_e}\frac{Nu \cdot k}{d}(T - T_p)$$

where the shape function for parcel p associated with the node k is ϕ_k, the number of particles in parcel p is N_p, the area of the host element is A_e, the Nusselt number is Nu and the thermal conductivity of the gas is k, where u, T, d, u_p, and T_p are the gas velocity and temperature, the particle diameter, velocity, and temperature, respectively, and the subscript i indicates the direction of the velocity in a Cartesian coordinate system and where a conventional C_D formulation given by Clift et al.[8] (as opposed to an unsteady formulation) was shown to yield robust predictive performance for dusty shock attenuation.[1] The parcel shape functions are then used to scatter each parcel's contributions to the host element's nodes; thus, parcel coupling terms within the elements connected to any node are summed in a linear weighting fashion to that node. Further details on the formulation can be found in Sivier et al.[9] The Lagrangian parcel equations[7,10] are then solved with an explicit single-step finite difference formulation for each parcel to update the parcel unknowns. The Lagrangian description involved continuously determining the host element once a parcel had moved or when the unstructured mesh was refined/coarsened. The use of a vectorized successive neighbor search[11] was found to provide an elegant and efficient solution to this problem.

A novel technique was used to make the parcels adapt to the dynamic element distribution by sensing the local parcel population. To locally determine if a refinement or a coarsening of parcels is to be performed, the number of parcels in each element is noted following each mesh refinement. If there are fewer than some preset

Received July 20, 1994; revision received June 27, 1995; accepted for publication June 28, 1995.

*Graduate Research Assistant, Department of Aeronautical and Astronautical Engineering. Student Member AIAA.

†Associate Professor, Department of Aeronautical and Astronautical Engineering. Senior Member AIAA.

‡Senior Research Scientist. Associate Fellow AIAA.

§Research Professor, CSI. Member AIAA.

number (P_{min}) of parcels in a given element, then the largest parcel (by number of particles) in that element is divided into some preset number (P_{ref}) of parcels, each containing an equal number of particles. These parcels are then distributed around the original parcel.[9] A baseline distribution distance (Δh_b) was based on separating the new parcels by approximately one-sixth of an element face, which corresponded to 0.28 of the square root of the element area. P_{ref} was chosen as five to allow the retention of the original parcel location as well as a distribution of four new parcels in each Cartesian direction. The temperatures and velocities of the new parcels are simply set equal to that for the original parcel to satisfy momentum and energy conservation. Such a scheme results in some numerical diffusion of the particle concentration. If there are more parcels in a given element than some preset number (P_{max}), then a preset number (P_{coar}) of the smallest parcels in that element are combined to form one larger parcel. The characteristics (temperature and velocity) for the new parcel are conservatively determined by a mass weighted average of the characteristics of the old parcels.[9]

III. Discussion

As a test flow, the described techniques have been applied to the case of a right-running shock with an initial shock speed of 1.48 as it passes through a 5 cm high by 420 cm long domain that contains 27-μm glass particles with a density of 2.5 g/cm^3 suspended in a quiescent air with a mass loading (η, ratio of particle mass of gas mass in a unit volume of gas) of 1.25, which corresponds to one of the test conditions of Sommerfeld.[4] A number of tests were run with the E–L code for which the number of initial parcels per cell was varied. The shock was allowed to propagate roughly 40 cm from its original position. In all of the tests, the parcels were initialized in the elements in a cell structured manner, no parcel refinement/coarsening was used, and the mesh was allowed to refine to three levels (LOR = 3), with a background cell size of about 1.25 cm.

For the first case, each element was initialized with only one parcel (which represents roughly 29,600 particles) per element cell, where no elements were refined in the initial particle laden region. This very coarse parcel distribution exhibits a great deal of noise in the gas density upstream of the shock wave in what should be an essentially one-dimensional shock wave attenuation (Fig. 1a). The second case initialized the flowfield with four parcels/element. The noise in the solution for this case was substantially reduced, however, some residual noise exists upstream of the shock (where the mesh refinement has reduced the parcel distribution to less than one parcel/element) and a nonphysical plateau in density is found just upstream of the shock (Fig. 1b). For the final case, the flow was initialized with 64 parcels/element, which is sufficient to maintain at least one parcel/element even at the finest mesh resolution (three levels). The noise in the solution has been reduced even further, and the density plateau is now absent upstream of the shock (Fig. 1c). This improvement in the solution, however, is very costly in computational resources due to the vastly increased number of parcels. For example, increasing to five levels of mesh refinement without parcel adaptivity would require more than 1000 parcels per background element. Therefore, these tests demonstrate a need for parcel refinement and coarsening when adaptive grids are used.

A number of tests were performed to study the effect of the initial parcel placement within the elements on the solution (cell centered, Cartesian based, and random). Sivier et al.[9] demonstrated that the best performance was realized when the parcels were initialized in a cell structured manner (i.e., the parcels were initialized symmetrically within each elements using a constant set of linear shape functions). This is because the placement of parcels that are symmetric with respect to the nodes of the cell yields the most accurate nodal contributions of the interphase coupling.

To allow a nearly constant (and thus efficient) number of parcels per host cell as the unstructured grid is refined and coarsened, the parcel-adaptive method was investigated to evaluate and optimize the characteristic parameters (P_{min}, P_{max}, Δh). The target range of parcels was varied to determine the optimal range that balances flow accuracy and computational efficiency. An example calculation of density contours with parameters (2, 7, Δh_b) is shown in Fig. 1d with a corresponding parcel distribution shown in Fig. 1e, where one may note the cell centered initial parcel distribution in front (to the right) of the shock. Along the shock itself, we note both cell and parcel refinement, which are subsequently both coarsened after the shock passes. Several different ranges of P_{min}, P_{max}, and Δh were tested,[9] and the results show that $P_{min} = 4$, $P_{max} = 9$, and Δh_b give the most satisfactory results.

The E–L technique with the cited parameters was compared with the E–E technique for the same case of a shock moving at an initial Mach number $M_0 = 1.48$, and with an initial particle loading of $\eta = 1.25$, as given by the experimental test conditions of Sommerfeld.[4] The E–L case had an average of 5000 elements and 28,000 parcels at any given time and used a timestep of about 0.12 μs based on the same conventional stability constraints used in the E–E technique.[1] The results of the shock speed attenuation over distance traveled through the particles are shown in Fig. 2 for

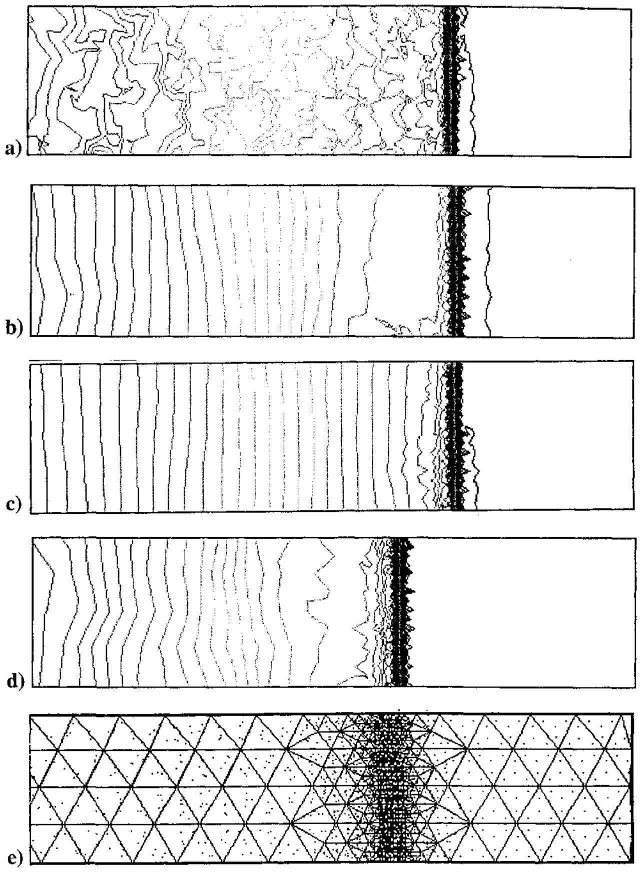

Fig. 1 E–L instantaneous results for gas density contours: a) without parcel adaptivity and initialized with 1 parcel/element, b) without parcel adaptivity and initialized with 4 parcel/element, c) without parcel adaptivity and initialized with 64 parcel/element, d) with parcel adaptivity and parameters (2, 7, Δh_b), and e) corresponding cell and parcel distribution.

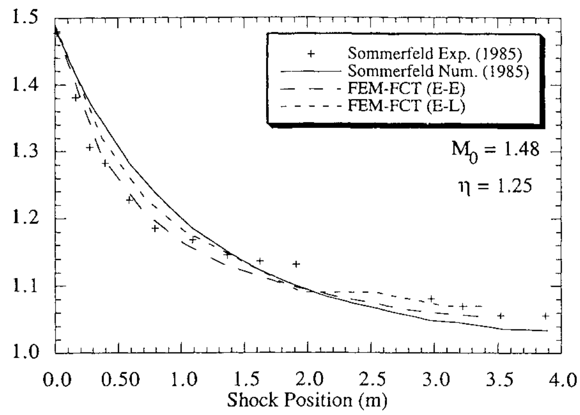

Fig. 2 Comparison between numerical and experimental data for shock attenuation.

both the E–E case and the E–L case [which was initialized with four parcels/cell and using the optimum parcel adaptivity parameters of (4, 9, Δh_b)]. Both cases used an LOR of 5 and yielded good correlation with experimental results, however, the E–E case exhibited better agreement and its density contours were found to be less noisy. The E–E case also required roughly a factor of two less CPU time (145 vs 337 min) and memory (1.3 vs 2.1 Mwords) on a Cray Y-MP than the E–L case.[9] Computational requirements were estimated for a hypothetical case that used the E–L technique also with an LOR of 5 but without adaptive parcels and with enough initial parcels to ensure one per cell at the highest refinement level. The resulting E–L case without parcel adaptivity required far more CPU time and memory (2900 min and 50.8 Mwords) than its equivalent parcel-adaptive E–L counterpart. This shows the strong potential for the parcel adaptivity scheme, especially as one progresses to three-dimensional flows. From these comparisons and results of Sivier et al.,[1,9] however, the E–E technique is the most computationally efficient for shock attenuation of this particular flowfield.

IV. Conclusions

A novel Lagrangian parcel-adaptive method has been developed and added to a two-phase compressible flow solver to allow a more accurate and more efficient study of particle and droplet flows. The flow computations employ the FEM–FCT scheme, while the finite difference Lagrangian parcel equations are solved directly for each parcel. The performance of the scheme under different implementations was evaluated using a test case of an unsteady shock attenuation in a dusty gas. The parcel adaptivity allowed an order of magnitude savings in computational resources as compared to a nonadaptive parcel treatment and was most effective when cell structured initialization was used along with an optimum refinement distribution length scale and optimum limits on the parcels per cell. The adaptive Lagrangian treatment of particles computational characteristics, however, was not as efficient as when the particle phase was treated in an Eulerian manner.

Acknowledgments

This research was supported by Science Applications International Corporation under Contract 21900208-82. Computer time was furnished by the National Center for Supercomputing Applications (NCSA) at University of Illinois Urbana–Champaign under Contract CBT900010N. The authors would like to acknowledge assistance from former undergraduate research assistant Cheryl Secora.

References

[1]Sivier, S., Loth, E., Baum, J., and Löhner, R., "Unstructured Adaptive Remeshing Finite Element Method for Dusty Shock Flow," *Shock Waves*, Vol. 4, No. 1, 1994.

[2]Faeth, G. M., "Mixing, Transport and Combustion in Sprays," *Progress in Energy and Combustion Science*, Vol. 13, 1987, pp. 293–345.

[3]Crowe, C. T., "REVIEW—Numerical Models for Dilute Gas-Particle Flows," *Journal of Fluid Engineering*, Vol. 104, Sept. 1982, pp. 297–303.

[4]Sommerfeld, M., "The Unsteadiness of Shock Waves Propagating Through Gas-Particle Mixtures," *Experiments in Fluids*, Vol. 3, 1985, pp. 197–206.

[5]Olim, Igra, Mond, and Ben-Dor, "A General Attenuation Law of Planar Shock Waves Propagating into Dusty Gases," *Proceedings of the 16th International Symposium on Shock Waves and Shock Tubes*, 1985, pp. 217–225.

[6]Dukowicz, J. K., "A Particle-Fluid Numerical Model for Liquid Sprays," *Journal of Computational Physics*, Vol. 35, 1980, pp. 229–253.

[7]Sommerfeld, M., "Numerical Simulation of Supersonic Two-Phase Gas-Particle Flows," *Proceedings of the 16th International Symposium on Shock Tubes and Waves*, 1987, pp. 235–241.

[8]Clift, R., Grace, J. R., and Weber, M. E., *Bubbles, Drops, and Particles*, Academic, New York, 1978, pp. 111–112.

[9]Sivier, S., Loth, E., Baum, J., Löhner, R., and Secora, C., "Dusty Shock Simulations with an Unstructured Grid and Adaptive Lagrangian Particles," AIAA Paper 94-2362, June 1994.

[10]Rudinger, G., "Flow of Solid Particles in Gases," AGARDograph 222, Oct. 1976.

[11]Löhner, R., and Ambrosiano, J., "A Vectorized Particle Tracer for Unstructured Grids," *Journal of Computational Physics*, Vol. 91, No. 1, 1990, pp. 22–31.

Transonic Equivalence Rule Involving Lift and Shocks

H. K. Cheng* and Shijun Luo†
University of Southern California,
Los Angeles, California 90089-1191

Introduction

FOR aerodynamic configurations with sufficiently high lift, the transonic equivalence rule[1–4] must be modified for both linear and nonlinear lift contributions.[5–11] The latter analyses show that for a thin wing having swept leading edges, with smooth lift and thickness distributions, the outer-flow region has a nonlinear structure determined principally by an equivalent line source and a line doublet. Apart from serving as a helpful guide to conceptual aerodynamic design, the equivalence rule and its extension can be useful in transonic wind-tunnel wall corrections, as well as studying sonic-boom impact at low-supersonic flight speed.

The present article re-examines the inner and outer solutions and their matching and clarifies the accuracy levels of the theory with consideration of the higher order corrections and shock discontinuities in the outer flow. The matching involving shocks in the outer flow (to be distinguished from a shock imbedded and terminated within the inner region), as shown by Cole and Malmuth[12] and Malmuth[13] for the axisymmetric case, leads to requirements on the local shock geometry and its location that may, in turn, determine their admissibility. Certain classes of admissible solution behavior and the open issues are noted.

Inner Solution in the Outer Limit: Corrections

The perturbation velocity potential ϕ in the inner region not far from the wing/body cross section $[r/b = \mathcal{O}(1)]$ is assumed to be expandable in the small parameter $\epsilon = [(\gamma + 1)M_\infty^2 \tau\lambda^3]^{1/2}$, as (cf. Ref. 5)

$$\phi/\alpha U b = \varphi_I + \epsilon\varphi_{II} + \epsilon^2\varphi_{III} + \epsilon^3\varphi_{IV} \tag{1}$$

where $\lambda \equiv b/l$, α is an effective attack angle, τ is a characteristic cross-section thickness ratio, b is a reference spanwise length scale, and l is a reference streamwise length scale. For the present purpose, only the first two terms are of concern, which can be decomposed into five parts φ_0, φ_1, φ_2, ψ_2, and ψ_2' as[5]

$$\varphi_I = \varphi_0, \qquad \varphi_{II} = \sigma_1^{-1}\varphi_1 + \tfrac{1}{8}\sigma_1\left(\varphi_2 + \Gamma\psi_2 + \Gamma^2\psi_2'\right) \tag{2}$$

with

$$\sigma_1 \equiv (\gamma + 1)^{\frac{1}{2}} M_\infty \lambda^{\frac{3}{2}} \alpha/\tau^{\frac{1}{2}}, \qquad \Gamma \equiv 8(\gamma + 1)^{-1}\lambda^{-2} \tag{3}$$

The results for φ_0, φ_1, φ_2, ψ_2, and ψ_2' presented in Eqs. (3.18), (3.19), (3.21), (3.22), and (3.24) of Ref. 5 need corrections for transcribing and printing errors. The corrected inner solution ϕ for large r is written in the outer variable $\eta = \epsilon r$, omitting term of order $\epsilon^2\eta^{-2}$, $\epsilon^2\eta^{-1}$, $\epsilon^2 \ell n\, \epsilon$, ϵ^2, η as

$$\phi/\tau U b \equiv \Phi \sim (2\pi)^{-1} S_e'(x)\,\ell n\, \eta + (2\pi)^{-1}\sigma_1 F(x)\eta^{-1}\sin\omega + \beta_0(x) + \epsilon(2\pi)^{-1}\left[\tilde{D}_1(x)\eta^{-1}\cos\omega + \sigma_1 m_{32}\eta^{-2}\sin 2\omega\right] + \Phi_{\mathrm{non}} \tag{4}$$

with

$$\sigma_*^2 = \sigma_1^2\,|\ell n\, \epsilon| \tag{5}$$

Received Sept. 6, 1994; revision received July 19, 1995; accepted for publication July 19, 1995.

*Professor Emeritus, Department of Aerospace Engineering. Fellow AIAA.

†Visiting Professor, Department of Aerospace Engineering; on leave from Northwestern Polytechnical University, Xi'an, People's Republic of China.